Synthesis and Molecular Structure of Highly Compact Star-Like Poly(Methyl Methacrylate) and Poly(Butyl Methacrylate)

H. Mahmoud Aboelanin,[a,b] *S. Podzimek,*[a,c,d*] *V. Spacek* [d]

[a] Institute of Chemistry and Technology of Macromolecular Materials, University of Pardubice, 53210 Pardubice, Czech Republic

[b] Department of Chemistry, Faculty of Science, Al-Azhar University, 11884 Cairo, Egypt

[c] Wyatt Technology Europe, D-56307 Dernbach, Germany

[d] SYNPO, 53207 Pardubice, Czech Republic

*Email: stepan.podzimek@synpo.cz

Keywords: Star-like polymers, group transfer polymerization, size exclusion chromatography, multi-angle light scattering, online viscometry

ABSTRACT

Poly(methyl methacrylate) and poly(*n*-butyl methacrylate) highly dense star-like polymers with a varied number and length of arms were prepared by the arm-first group transfer polymerization. The refractive index increment of the star-like polymers was compared with that of corresponding linear homopolymers. The prepared polymers were characterized by size exclusion chromatography coupled with a multi-angle light scattering detector and an online viscometer. Except for the commonly used molar mass, root mean square radius, and intrinsic viscosity, the obtained data also allowed the determination of the distribution of the arms per molecule, the calculation of the average number of arms per molecule, and the determination of the molar mass dependency of the draining factor. The relation between the number of arms per molecule and

molar mass was estimated using various theoretical equations and compared with the true values obtained by the division of the slice molar mass by the molar mass of arms.

Introduction

Branched polymers are interesting for researchers from various application areas, as the presence of branches results in different physical properties compared to linear analogues.[1] Star-like polymers are one of several types of branched polymers. They consist of multiple arms radiating from the central core.[2] Highly compact star-like homopolymers of methyl methacrylate and butyl methacrylate and their analogues with hydroxy, carboxy, or epoxy functionality can serve for the enhancement of mechanical properties of paints, adhesives, or composites.[3] Star-like polymers have been widely studied because of their unique topological structures and attractive physical and chemical properties. Therefore, a number of researchers have focused on star polymers to design various advanced materials for biomedical applications, including drug and gene delivery, diagnosis, antibacterial and antifouling coatings, and implanted medical devices.[4-8] A potential advantage of the highly compact star-like structures is that their addition to liquids results in a moderate increase of viscosity.[9] They can also serve as models for investigating and understanding the properties of other star-like structures used in drug-delivery,[10] catalysis,[11] and semiconductor technologies.[12] The molar mass distribution and the distribution of arms per molecule are crucial for the application properties.

The classical branching paper by Zimm and Stockmayer[13] offers the following equations relating the number of arms (f) with the branching ratio (g):

$$g = \frac{6f}{(f+1)(f+2)} \quad (1)$$

$$g = \frac{3f-2}{f^2} \tag{2}$$

Equation 1 was derived for star polymers where the arm length is polydisperse, i.e., the arms are not of equal length, whereas Equation 2 was derived for the stars with equal arm length. The branching ratio (contraction factor) is defined as the ratio of the mean square radii of branched (*br*) and linear (*lin*) molecules of the same molar mass (M) :

$$g = \left(\frac{R_{br}^2}{R_{lin}^2}\right)_M \tag{3}$$

where R is the root mean square (RMS) radius (radius of gyration) and the subscript M indicates that the comparison is performed for the macromolecules of equal molar mass. A general limitation of the above equations is that they are valid for theta conditions, whereas the SEC measurements are typically performed in thermodynamically good solvents. As the thermodynamic quality of the solvent decreases with increasing degree of branching, the expansion of the branched macromolecules in thermodynamically good solvent is less than that of linear polymer chains. Consequently, the experimental values of g become smaller compared to the theta state.

Alternative branching ratio based on the intrinsic viscosity ($[\eta]$) was suggested by Zimm and Kilb:[14]

$$g' = \left(\frac{[\eta]_{br}}{[\eta]_{lin}}\right)_M \tag{4}$$

The two branching ratios are related by a simple equation:

$$g' = g^e \tag{5}$$

The main limitation is given by the fact that the relation of g' to the number of arms in star polymers or number of branch units in randomly branched macromolecules is less certain as it is

via the parameter *e* which is related to the drainability of polymer chains. The draining parameter *e* is supposed to fall in the range of 0.5 – 1.5, yet the exact value is mostly unknown.

Literature offers several equations relating the number of arms directly with the intrinsic viscosity-based branching ratio:[14-16]

$$g' = \frac{(2/f)^{1.5}[0.396(f-1)+0.196]}{0.586} \tag{6}$$

$$g' = \left(\frac{3f-2}{f^2}\right)^{0.58} \frac{0.724-0.015(f-1)}{0.724} \tag{7}$$

$$log\, g' = 0.36 - 0.8\, log\, f \tag{8}$$

The arm-first synthetic route offers a possibility of the calculation of the number of arms at each elution volume slice by dividing the slice molar mass by the molar mass of the arms prepared in the first step of polymerization. The obtained relation between the number of arms per molecule and molar mass allows testing various literature equations with the goal of finding the most appropriate one that would allow the determination of the arms per molecule–versus–molar mass plots for samples for which the arm molar mass is unknown (mostly commercial products or polymers prepared by other polymerization techniques). Note that the elution volume slices are not strictly monodisperse as they are affected by the band broadening. Moreover, in the case of branched polymers, the additional contribution to the slice polydispersity is a possible co-elution of macromolecules of identical hydrodynamic volume, yet of different branching degree, topology and molar mass. The latter effect should be negligible in the case of star polymers prepared from almost uniform arms. Nevertheless, the slice polydispersity must be neglected as there is no simple way of compensating for it.

Experimental

A group transfer polymerization (GTP) with the arm-first strategy was used for the preparation of poly(methyl methacrylate) (PMMA) and poly(*n*-butyl methacrylate) (PBMA) star-like polymers. Methyl trimethylsilyl dimethylketene acetal and tetrabutyl amonium acetate were used as the initiator and catalyst, respectively. Both reagents were dosed to a three-necked round bottom flask with tetrahydrofuran (THF) kept under the nitrogen atmosphere. The monomer was dosed dropwise under stirring for around 25 min. The reaction mixture was stirred for an additional 20 min after completing the monomer dosing. Next, about 10 mL sample solution was withdrawn from the reaction flask for the determination of the molar mass distribution of the arm. After that, the linking agent ethylene glycol dimethacrylate (EGDMA) was added slowly under stirring to form the star-like polymer. The solids of final THF solutions consisting of star-like structures and remaining arms were ≈ 50 wt. % (PBMA) and ≈ 40 wt. % for (PMMA). The molar ratios of particular reagents for all prepared samples are listed in Table 1. Linear PMMA and PBMA were prepared by solution free radical polymerization using 0.1 % wt. azobisisobutyronitrile as initiator. About 50 mL of 50 % solution of monomer in toluene was placed into a 100 mL closed vial and heated at 80 ºC for 8 hr. After completing the polymerization, the polymer solution was left to cool overnight. The solids of polymer solutions were ≈ 40 % (PMMA) and ≈ 32 % (PBMA). The polymers were precipitated by *n*-hexane and dried in a vacuum oven at 40 ºC to a constant weight.

The specific refractive index increment (*dn*/*dc*) was determined in THF at 25 ºC using a refractive index (RI) detector Optilab T-rEX operating at 660 nm (Wyatt Technology). The determination was performed off-line by injecting six THF solutions of concentration ranging from ≈ 0.3 mg/mL to ≈ 5 mg/mL. The stars for the *dn*/*dc* measurements were isolated from the unreacted arms by the precipitation of THF solutions resulting from GTP by *n*-hexane and subsequent drying

in a vacuum oven at 40 °C. The arms were isolated by drying the solutions obtained after the first polymerization step before addition of EGDM. The star purity was checked by conventional size exclusion chromatography (SEC) with an RI detector. An Alliance e2695 Separation Module with a 2414 RI detector (both Waters) and two Agilent Mixed-C 300 × 7.5 mm 5 μm columns with THF at 1 mL/min were used for this purpose. All stars contained less than ≈ 2 wt. % of remaining arms.

The molar mass distributions, the conformation plots (RMS radius versus molar mass), and the Mark-Houwink plots were determined by SEC with a multi-angle light scattering (MALS) detector DAWN NEON, an RI detector Optilab NEON and an online viscometer ViscoStar NEON (all detectors from Wyatt Technology). The SEC system consisted of a 1200 Series isocratic pump and autosampler with two Mixed-C 300 × 7.5 mm 5 μm columns (all Agilent Technologies) using THF as the mobile phase at a flow rate of 1 mL/min. Samples were prepared at concentrations of ≈ 2.5 mg/mL (stars and linear homopolymers), ≈ 5 mg/mL (long arms), and ≈ 10 mg/mL (short arms). The samples were filtered with 0.45 μm filters and injected in the amount of 100 μL. The data collection and processing were performed by Wyatt Technology software ASTRA. In addition to the calculations and plots provided by ASTRA, the data were exported from ASTRA as csv files for additional processing in Excel.

Table 1 Molar ratios of reagents used for the synthesis of star-like PMMA and PBMA

Sample	Monomer	Molar ratio		
		Initiator	Monomer	EGDMA
M1	MMA	1	30	1.3
M2	MMA	1	30	1.5
M3	MMA	1	30	1.8
M4	MMA	2.5	30	2.3
M5	MMA	2.5	30	4.0
B1	BMA	1	49	1.7
B2	BMA	1	49	2.8
B3	BMA	1	49	3.7
B4	BMA	4	49	8.4
B5	BMA	4	49	9.3

Results and Discussions

The number-average (M_n) and the weight-average (M_w) molar masses, the values of dispersity ($Đ$), and the weight-average intrinsic viscosities ($[\eta]_w$) of arms and stars, and the star fractions in the final polymerization products for several star-like PMMA and PBMA are listed in Tables 2 and 3, respectively. The samples were selected to cover different molar mass and/or arm length. The constants of Mark-Houwink equation as well as the parameters of the conformation plot for linear PMMA and PBMA are summarized in Table 4. They were used for the calculation of g and $g´$ ratios.

Table 2 The values of M_n, M_w, $Đ$, $[\eta]_w$, and star fraction for star-like PMMA

Sample	M_n (10^3 g/mol)	M_w (10^3 g/mol)	$Đ$	$[\eta]$ (mL/g)	Star fraction (%)
M1 arm	6.5	6.9	1.07	6.1	–
M1 star	66	102	1.54	11.2	77
M2 arm	6.5	7.0	1.08	6.1	–
M2 star	147	267	1.82	11.7	73
M3 arm	6.4	6.9	1.08	6.1	–
M3 star	273	606	2.22	12.4	76
M4 arm	1.9	2.1	1.09	3.7	–
M4 star	21	47	2.28	6.6	76
M5 arm	1.9	2.1	1.07	3.8	–
M5 star	84	388	4.62	8.9	87

Table 3 The values of M_n, M_w, $Đ$, $[\eta]_w$, and star fraction for star-like PBMA

Sample	M_n (10^3 g/mol)	M_w (10^3 g/mol)	$Đ$	$[\eta]$ (mL/g)	Star fraction (%)
B1 arm	7.3	7.7	1.06	5.7	–
B1 star	61	111	1.81	10.7	62
B2 arm	8.8	9.9	1.12	6.5	–
B2 star	377	610	1.62	13.0	68
B3 arm	8.9	9.3	1.05	6.1	–
B3 star	550	1132	2.06	13.6	74
B4 arm	2.5	2.7	1.10	3.8	–
B4 star	117	329	2.83	9.1	82
B5 arm	2.4	2.7	1.11	3.8	–
B5 star	237	1712	7.22	12.8	87

Table 4 Mark-Houwink constants and parameters of conformation plot for linear PMMA and PBMA (THF, 25 °C, averages from six measurements)

Polymer	Mark-Houwink plot		Conformation plot	
	K (10^{-3} mL/g)	a	k (nm)	b
PMMA	10.6 ± 0.5	0.701 ± 0.003	0.016 ± 0.002	0.566 ± 0.008
PBMA	7.24 ± 0.4	0.732 ± 0.005	0.011 ± 0.001	0.593 ± 0.005

The specific refractive index increment is needed for the accurate calculation of molar mass from the combined MALS and RI detection and for the determination of intrinsic viscosity from RI detector and viscometer. Table 5 compares the values of *dn*/*dc* for linear polymers, stars and arms. The values for linear polymers are well comparable with those reported previously.[17,18] The highly dense structure of star-like polymers does not have a significant impact on *dn*/*dc*. As expected, the *dn*/*dc* values are lower for the arms as a consequence of their low molar mass.

Table 5 Specific refractive index increments of PMMA and PBMA stars, arms, and linear polymers (THF, 25 °C, 660 nm)

Polymer	M_w (10^3 g/mol)	*dn*/*dc* (mL/g)*
PMMA linear	310 and 606	0.084 ± 0.001
PMMA star	53 and 381	0.082 ± 0.002
PMMA arm	6.9	0.077 ± 0.001
PMMA arm	2.1	0.074 ± 0.001
PBMA linear	497	0.077 ± 0.002
PBMA star	201 and 639	0.080 ± 0.002
PBMA arm	7.7	0.072 ± 0.001
PBMA arm	2.7	0.069 ± 0.001

*Average from (top to bottom) 5, 4, 4, 2, 5, 5, 4, and 2 measurements. The uncertainty is based on standard deviation and the uncertainty reported by ASTRA software.

Figure 1 depicts typical molar mass versus elution volume plot of one of the star-like PMMA together with the plot of the arm synthetized in the first step. The data prove the ability of modern MALS detector to yield sufficient signal to determine the molar mass down to proximity of a thousand g/mol. It must be emphasized at this point that flushing the SEC columns for at least several hours is of utmost importance to minimize the noise caused by the particles bleeding from column packing. The proper flushing is necessary after each restart of the pump since pressure change releases the particles that were trapped in the columns during the previous runs. Figure 1 also shows that the stars can be well separated from the original arms which allows their quantification and characterization without isolation from the remaining arms. The conformation and Mark-Houwink plots of the same sample are shown in Figure 2 together with the plots of linear PMMA for comparison. Data from Figure 2 yield the molar mass dependency of the ratios g and g' shown in Figure 3. The draining parameter e can be calculated by comparing the branching ratios g and g' at the same molar mass. The relation between the parameter e and molar mass is described in Figure 4 together with that obtained for one of star-like PBMA. The values of e from ≈ 0.5 to ≈ 1.2 fall in the expected range and confirm the dependence of the draining parameter on molar mass. The increase of parameter e with molar mass indicates increasing drainability of large star-like macromolecules.

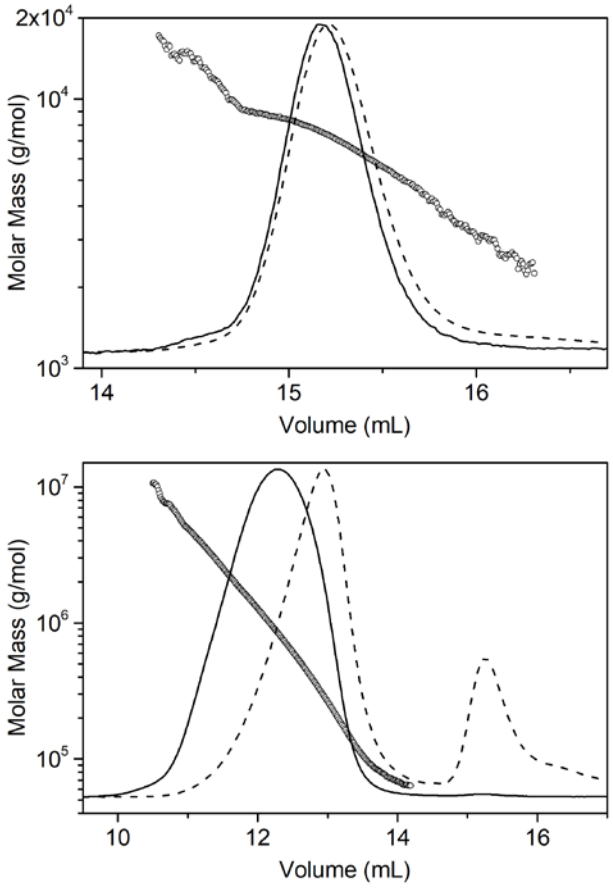

Figure 1 Molar mass versus elution volume plots of arm (top) and star-like PMMA (bottom) (sample M3). MALS @ 90° (solid) and RI (dashed) chromatograms are overlaid.

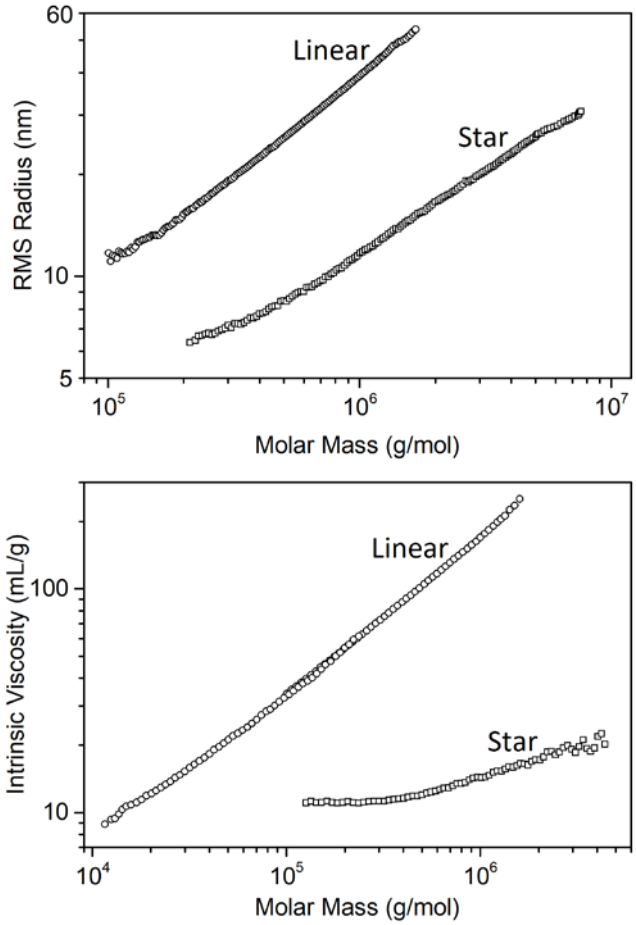

Figure 2 Conformation (top) and Mark-Houwink (bottom) plots of linear PMMA and star-like PMMA (sample M3).

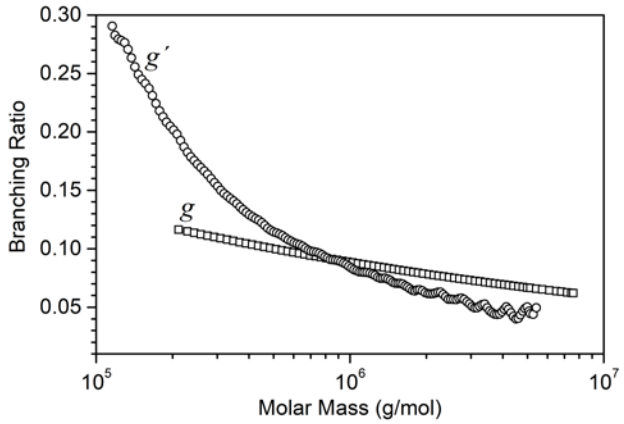

Figure 3. Branching ratios g (□) and g' (○) versus molar mass plots of star-like PMMA (sample M3).

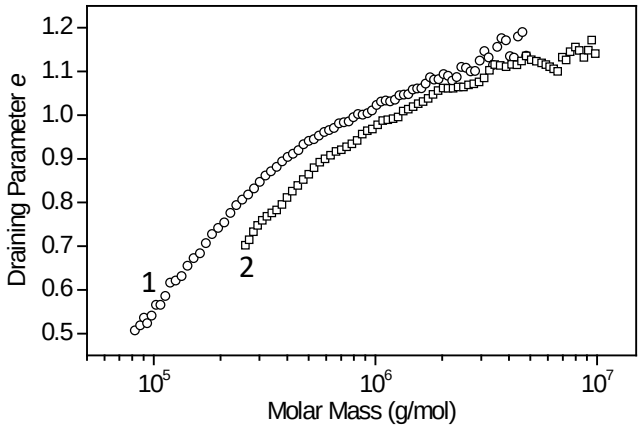

Figure 4 Draining parameter *e* versus molar mass plots of star-like PMMA (1, ○) and PBMA (2, □) (samples M3 and B3).

The conformation plot is the most direct way to branching information. However, it has two limitations. It cannot be applied to polymers composed of the majority of molecules with RMS radii below ≈ 7 nm. Moreover, for many branched polymers it is strongly affected by the delayed elution of branched macromolecules as described for example in Reference.[19] The size limit applies to most of the prepared samples due to very high molecular compactness. In contrast to the conformation plot, the Mark-Houwink plot can be reliably measured with practically no size limit. In addition, it is markedly less affected by the delayed elution of the branched macromolecules.[20]

Mark-Houwink plots of several star-like PMMAs composed of different arm length are compared in Figure 5. The slope (Mark-Houwink exponent) of the plots of star-like polymers consisting of long arms is close to zero at the region of lower molar masses, which indicates sphere-like structure. Towards the high molar masses, the slope increases to the value of ≈ 0.28. The slope of the plots of samples consisting of short arms starts at ≈ 0.1 and increases to the same value as that of the stars from long arms. At lower molar masses, the plots of stars created by short arms are shifted to lower intrinsic viscosities which can be explained by higher number of arms at the same molar mass and thus more compact molecular structure. The difference diminishes towards

high molar masses, likely due to the change to more expanded structure for which the difference due to different arm length diminishes. The same explains the increase of the slope.

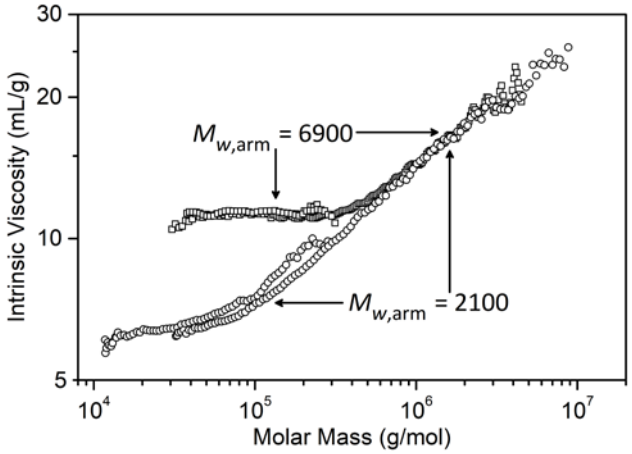

Figure 5. Mark-Houwink plots of star-like PMMAs with arm $M_w \approx 2100$ g/mol (○) and ≈ 6900 g/mol (□).

The obtained data allow testing various *g*–versus–*f* equations since the true number of arms at each molar mass can be calculated from the slice molar mass and molar mass of the arm prepared in the first reaction step. Instead of explicitly expressing the *f* as a function of *g* or *g´*, Equations 1, 2, 6, 7, and 8 were entered into Excel, and *g* or *g´* were calculated for the stepwise increasing *f*, and then the experimental values of *g* or *g´* were matched in regular intervals with *f*. Figure 6 depicts various plots of the number of arms per molecule against molar mass for star-like PMMA sample for which the determination of the RMS radius was possible and which did not show a significant tendency to the delayed elution and such allowed testing also the Equations 1 and 2. The conclusion from Figure 6 is that none of the equations allow accurate determination of the number of arms from the ratios *g* or *g´*. However, a very good agreement between the plot obtained using Equation 6 and that calculated from the slice molar mass was obtained for stars created by short arms as shown in Figure 7. The modification of Equation 6 in the sense of using exponent

1.6 instead of 1.5 gives good agreement for the stars consisting of long arms as shown in Figure 8. Similar results are obtained for star-like PBMA, i.e., Equation 6 markedly overestimates the number of arms per molecule in the case of long arms, whereas markedly better agreement is obtained for polymer consisting of short arms as shown in Figure 9. The polymer consisting of long arms requires increasing the exponent to the value of ≈ 1.7 as demonstrated in Figure 10. Comparison of samples M3 (arm M_w ≈ 6900 g/mol) and B3 (arm M_w ≈ 9300 g/mol) indicates that longer arms require higher exponent.

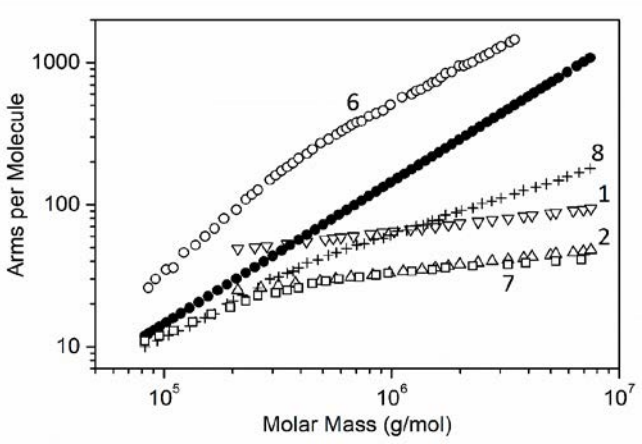

Figure 6 Plots of number of arms per molecules versus molar mass calculated by the division of slice molar mass by M_w of arms (●) and estimated from Equations 1, 2, 6, 7, and 8 for star-like PMMA with arm M_w ≈ 6900 g/mol (sample M3).

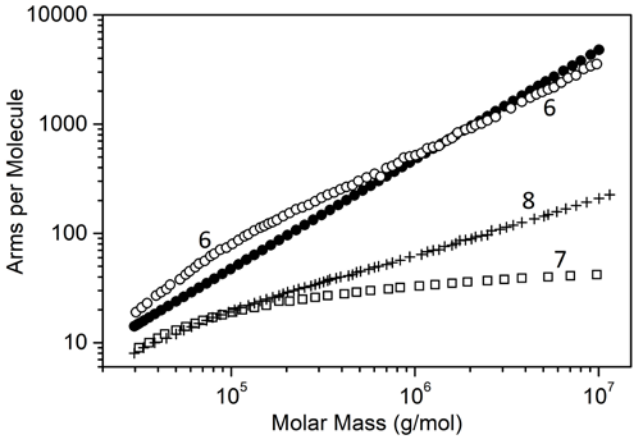

Figure 7 Plots of number of arms per molecule versus molar mass calculated by the division of slice molar mass by M_w of arms (●) and estimated from Equations 6, 7, and 8 for star-like PMMA with arm $M_w \approx 2100$ g/mol (sample M5).

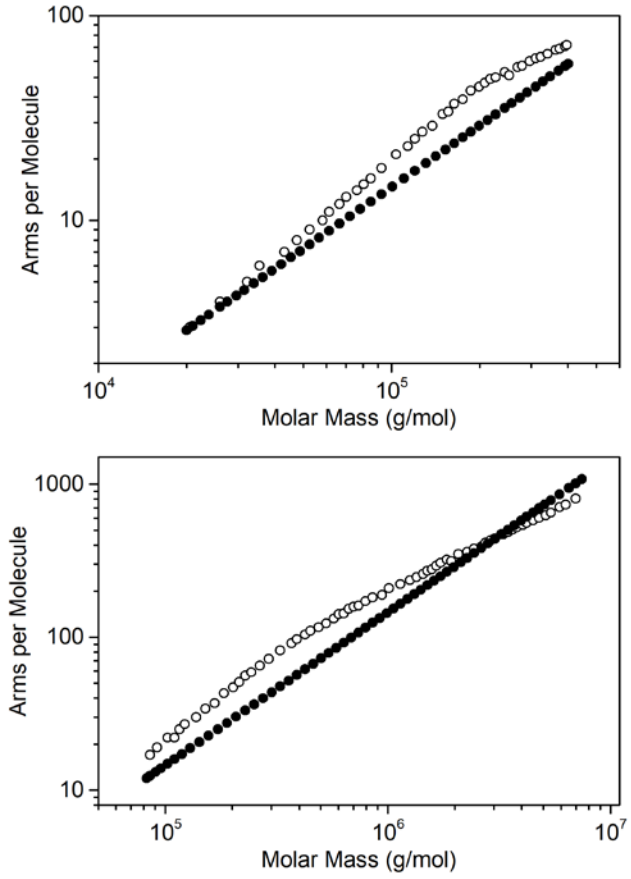

Figure 8 Plots of number of arms per molecule versus molar mass for two star-like PMMAs consisting of arms having $M_w \approx 6900$ g/mol calculated by the division of slice molar mass by M_w of arms (●) and estimated from Equation 6 using the exponent 1.6 instead of 1.5 (○, samples M1 top and M3 bottom).

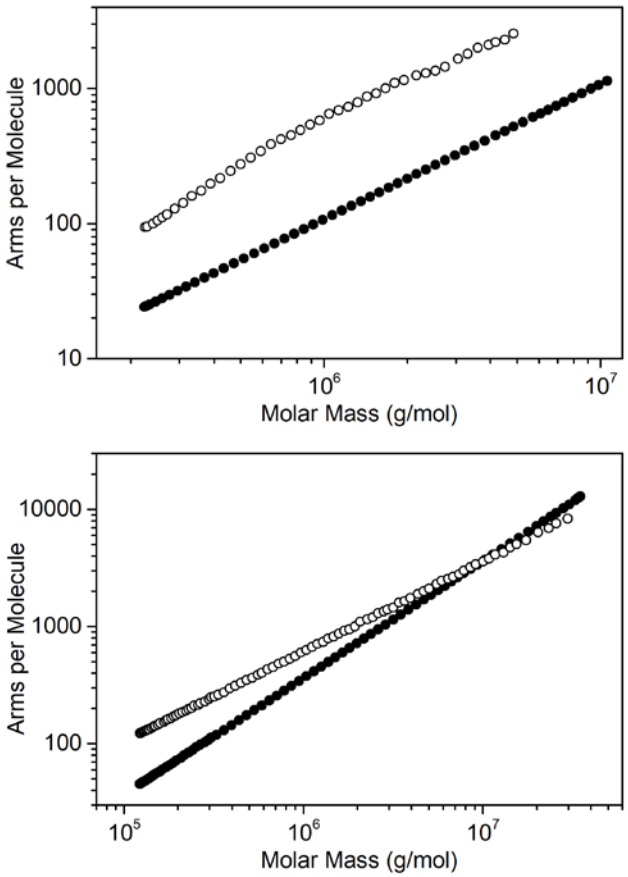

Figure 9 Number of arms per molecule versus molar calculated by the division of slice molar mass by M_w of arms (●) and estimated using Equation 6 (○) for star-like PBMA with arm $M_w \approx 9300$ g/mol (top, sample B3) and $M_w \approx 2700$ g/mol (bottom, sample B5).

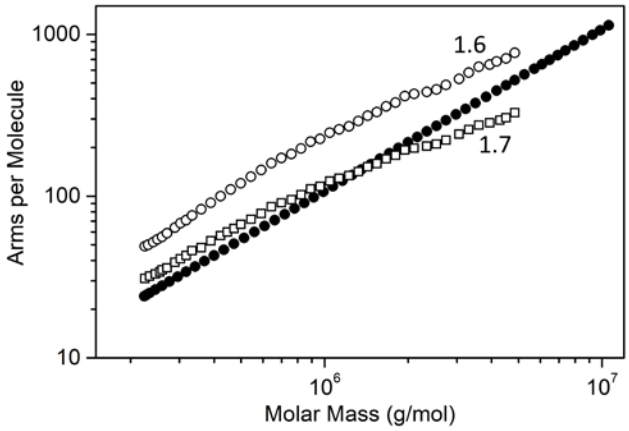

Figure 10 Plots of number of arms per molecule versus molar mass for star-like PBMA consisting of arms having $M_w \approx 9300$ g/mol calculated by the division of slice molar mass by M_w of arms (●) and estimated from Equation 6 using the exponent 1.6 (○) and 1.7 (□), (sample B3).

The molar mass distribution exported from ASTRA to Excel can be converted to the distribution of arms per molecule by dividing the molar mass axis by the molar mass of arm. The plots obtained for various PMMA and PBMA star-like polymers are shown in Figure 11.

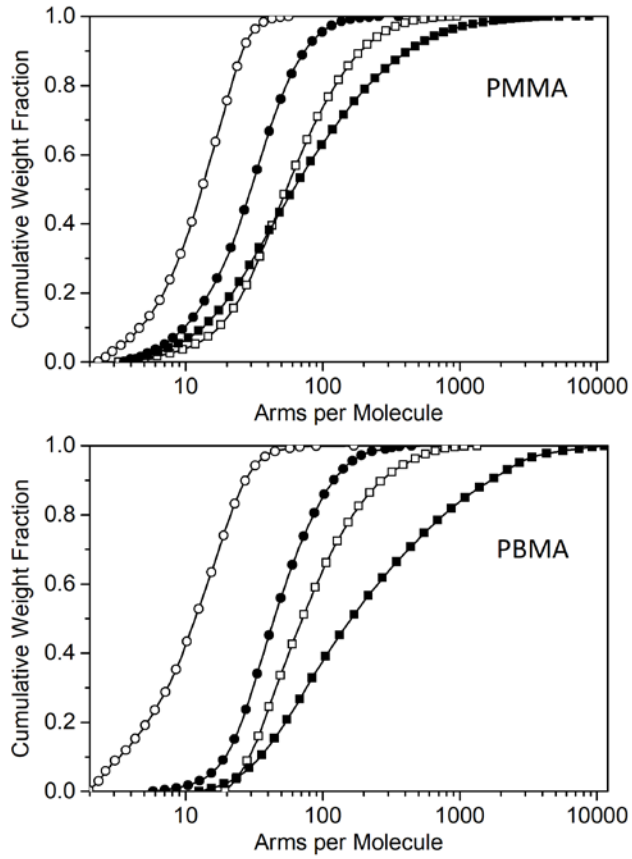

Figure 11 Cumulative distribution of arms per molecule for PMMA star-like polymers with long (samples M1 ○, M2 ●, and M3 □) and short (sample M5 ■) arms; and for PBMA star-like polymers with long (samples B1 ○, B2 ●, and B3 □) and short (sample B5 ■) arms.

Exporting the slice molar masses and the slice concentrations permits the calculation of the number-average (f_n) and the weight-average (f_w) arms per molecule using the equations equivalent to those for the calculation of molar mass moments:

$$f_n = \frac{1}{\sum \frac{w_i}{f_i}} \tag{9}$$

$$f_w = \sum w_i f_i \tag{10}$$

where f_i is the number of arms in molecules eluting at the *i-th* elution volume V_i and w_i is the weight fraction of molecules eluting at that V_i calculated as the slice concentration c_i divided by

the sum $\sum c_i$. The results for samples shown in Figure 11 are listed in Table 6. Table 6 is further completed by the values of $g´(M_w)$. The average branching ratio $g´(M_w)$ is the ratio of the experimental weight-average intrinsic viscosity of the branched polymer divided by the intrinsic viscosity of a hypothetical linear polymer that would have the same M_w as the polymer requiring analysis. This ratio can be used for mutual comparison of different samples for which the molar mass of arms is unknown.

Table 6 Number-average and weight-average arms per molecule and $g´(M_w)$ for samples shown in Figures 9 and 10

Sample	f_n	f_w	$g´(M_w)$
M1	9	24	0.326
M2	19	35	0.173
M3	35	80	0.103
M5	35	163	0.101
B1	8	13	0.300
B2	33	56	0.105
B3	52	110	0.069
B5	77	582	0.048

Conclusions

The arm-first GTP technique allows preparation of PMMA and PBMA star-like polymers in a wide range of arms per molecule and with different arm lengths. The knowledge of the absolute molar mass of arms prepared in the first step allows the determination of the true distribution of arms per molecule and the average values as well as the relation between *f* and molar mass. Most of the literature equations provide values of arms per molecule far from the true ones. The only exception is Equation 6 which is approximately valid for polymers consisting of short arms. In the case of long arms, Equation 6 needs to be slightly modified by increasing the exponent 1.5 to the values of 1.6 – 1.7. The obtained data suggest that the longer arms require a higher exponent. However, this finding is of limited practical meaning for polymers of unknown arm length that can be only compared mutually using the average ratio $g'(M_w)$. The impact of the highly dense molecular structure on the specific refractive index increment is negligible, whereas markedly lower values of *dn*/*dc* were found for the arms. The draining parameter of the star-like polymers was found to be molar mass dependent within the expected range of about 0.5 to 1.2.

AUTHOR INFORMATION

Corresponding Author

Stepan Podzimek – *Institute of Chemistry and Technology of Macromolecular Materials, University of Pardubice, 53210 Pardubice, Czech Republic; Wyatt Technology, D-56307 Dernbach, Germany; SYNPO, 53207 Pardubice, Czech Republic;* orcid.org/0000-0002-4741-3908*;* Email: stepan.podzimek@synpo.cz

Authors

Hamza Mahmoud Aboelanin – *Institute of Chemistry and Technology of Macromolecular Materials, University of Pardubice, 53210 Pardubice, Czech Republic; Department of Chemistry, Faculty of Science, Al-Azhar University, 11884 Cairo, Egypt;* orcid.org/0000-0003-2458-2044

Vladimir Spacek – *SYNPO, 53207 Pardubice, Czech Republic*

Notes

The authors declare no competing financial interest.

ACKNOWLEDGMENT

The authors acknowledge SYNPO for permitting all experiments in its laboratories, and Wyatt Technology for a long-term scientific cooperation and support.

REFERENCES

(1) Neelakandan, S.; Wang, L.; Zhang, B.; Ni, J.; Hu, M.; Gao, C.; Wong, W. Y.; Wang, L. Branched polymer materials as proton exchange membranes for fuel cell applications. *Polym. Rev.* **2022**, 62(2), 261-295.

(2) Higashihara, T.; Hayashi, M.; Hirao, A. Synthesis of well-defined star-branched polymers by stepwise iterative methodology using living anionic polymerization. *Prog. Polym. Sci.* **2011**, 36(3), 323–375.

(3) Pinto R.; Monastyreckis, G.; Aboelanin, H. M.; Spacek, V.; Zeleniakiene, D. Mechanical properties of carbon fibre reinforced composites modified with star-shaped butyl methacrylate. *J. Compos. Mater*. **2022**, 56(6), 951-959.

(4) Lapienis, G. Star-shaped polymers having PEO arms. *Prog. Polym. Sci.* **2009**, 34(9), 852–892.

(5) Kuckling, D.; Wycisk, A. Stimuli-responsive star polymers. *J. Polym. Sci. A: Polym. Chem.* **2013**, 51(14), 2980–9294.

(6) Iatridi, Z.; Tsitsilianis, C. Water-soluble stimuli responsive star-shaped segmented macromolecules. *Polymers* **2011**, 3(4), 1911–1933.

(7) Deng, Y.; Zhang, S.; Lu, G. L.; Huang, X. Y. Constructing well-defined star graft copolymers. *Polym. Chem.* **2013**, 4(5), 1289–1299.

(8) Mei, L.; Jiang, Y. Y.; Feng, S. S. Star-shaped block polymers as a molecular biomaterial for nanomedicine development. *Nanomedicine* **2014**, 9(1), 9-12.

(9) Martini, A.; Ramasamy, U. S.; Len, M. Review of viscosity modifier lubricant additives. *Tribol. Lett.* **2018**, 66, 1-14.

(10) Moorkoth, D.; Nampoothiri, K. M.; Nagarajan, S.; Girija, A. R.; Balasubramaniyan, S.; Kumar, D. S. Star-shaped polylactide dipyridamole conjugated to 5-fluorouracil and 4-piperidinopiperidine nanocarriers for bioimaging and dual drug delivery in cancer cells. *ACS Appl. Polym. Mater*. **2021**, 3(2), 737-756.

(11) Cheng, X.; Rong, L. H.; Peng-Fei Cao, P. F.; Advincula, P. Core–shell gold nanoparticle-star copolymer composites with gradient transfer and transport properties: toward electro-optical sensors and catalysis. *ACS Appl. Nano Mater.* **2021**, 4(2), 1394-1400.

(12) Sarvari, R.; Akbari-Alanjaraghi, M.; Massoumi, B.; Beygi-Khosrowshahi, Y.; Agbolaghi, S. Conductive and biodegradable scaffolds based on a five-arm and functionalized star-like polyaniline–polycaprolactone copolymer with ad-glucose core. *New J. Chem.* **2017**, 41(14), 6371-6384.

(13) Zimm, B. H.; Stockmayer, W. H. The dimensions of chain molecules containing branches and rings. *J. Chem. Phys.* **1949**, 17(12), 1301–1314.

(14) Zimm, B. H.; Kilb, R. W. Dynamics of branched polymer molecules in dilute solution. *J. Polym. Sci.* **1959**, 37(131), 19–42.

(15) Douglas, J.; Roovers, J.; Freed, K. Characterization of branching architecture through" universal" ratios of polymer solution properties. *Macromolecules* **1990**, 23(18), 4168–4180.

(16) Roovers, J. In Star and Hyperbranched Polymers, Mishra, M. K.; Kobayashi, S. Eds., *Marcel Dekker*; New York, NY, **1999**, p. 285.

(17) Simms, R. W.; Cunningham, M. F. High molecular weight poly (butyl methacrylate) by reverse atom transfer radical polymerization in miniemulsion initiated by a redox system. *Macromolecules* **2007**, 40(4), 860–866.

(18) Striegel, A. M. Specific refractive index increment (∂ n/∂ c) of polymers at 660 nm and 690 nm. *Chromatographia* **2017**,80(6), 989–996.

(19) Podzimek, S.; Vlcek, T.; Johann, C. Characterization of branched polymers by size exclusion chromatography coupled with multiangle light scattering detector. I. Size exclusion chromatography elution behavior of branched polymers. *J. Appl. Polym. Sci.* **2001**, 81(7), 1588–1594.

(20) Podzimek, S. Size Exclusion Chromatography, In Encyclopedia of Polymer Science and Technology, **2022**, DOI: 10.1002/0471440264.pst058.pub2.

For Table of Contents Only